Non-Hermitian Skin Effect: A Primer

Sagnik Seth,[1,*] Bihan Bhowmick,[2,†] and Himadri Barman[3,‡]

[1]*IISER Kolkata, Kolkata, India*

[2]*IISER Pune, Pune, India*

[3]*Department of Physics, Zhejiang University, Hangzhou 310027, China*

Hermiticity is a crucial condition for the observables to be real (hence measuarble) in our conventional quantum physics. However, the conventional quantum physics deals with the ideal scenario where the system is isolated from its environment. As soon as we take account of the interaction with the environment, we enter the generic world of non-equilibrium quantum physics where Hermiticity is not a required condition. The recent hunt of topological insulators for fault-tolerant quantum computation has opened the gate for studying the physics of non-Hermiticity into those materials. It has been recently discovered that non-Hermiticity induces an exotic phenomenon dubbed the *skin effect* which entails asymmetric localization of quantum states. In our article, we provide an introduction to this phenomenon and physics behind this with a flavor of students-friendly pedagogy.

CONTENTS

I. HATANO-NELSON MODEL: A FLAVOR OF NON-HERMITICITY IN A LATTICE

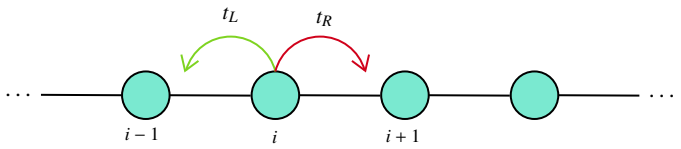

FIG. 1: Diagram showing the hopping in Hatano-Nelson Model

The Hatano-Nelson model (non-disordered) is the simplest tight-binding lattice model where the left and right-moving hopping amplitudes are unequal (*non-reciprocal*). The Hamiltonian for spinless particles in one dimension reads,

$$\hat{H}_{\mathrm{HN}} = \sum_{i=0}^{L-1} \left[t_R c_i^\dagger c_{i+1} + t_L c_{i+1}^\dagger c_i \right], \tag{1}$$

where L is the number of sites in the lattice and t_R and t_L are the right and left hopping amplitudes. The Hamiltonian is written using the second quantisation formalism, where c_i and $c_i^\dagger$ are the particle annihilation and creation operators at lattice site i, respectively. The Hamiltonian becomes non-Hermitian when $t_L \neq t_R$, that is, *asymmetric hopping*.

We can express the anihilation operator in the momentum space as:

$$c_i = \frac{1}{\sqrt{L}} \sum_{k=0}^{L-1} e^{ikx_i} c_k. \tag{2}$$

where x_i is the coordinate or position of site i. We then substitute this in the Hamiltonian:

$$\hat{H}_{\text{HN}} = \sum_L \sum_k \sum_{k'} t_R e^{-ikx_i} e^{ik'(x_i+a)} c_k^\dagger c_{k'} + t_L e^{-ik(x_i+a)} e^{ik'x_i} c_k^\dagger c_{k'} \tag{3}$$

$$= \sum_L \sum_k \sum_{k'} \left(t_R e^{ix_i(k'-k)} e^{ik'a} + t_L e^{ix_i(k'-k)} e^{-ika} \right) c_k^\dagger c_{k'} \tag{4}$$

$$= \sum_k \left(t_R e^{ika} + t_L e^{-ika} \right) c_k^\dagger c_k \qquad \left(\because \sum_i e^{i(k-k')x_i} = \delta_{kk'} \right) \tag{5}$$

$$= \sum_k E(k) c_k^\dagger c_k \tag{6}$$

where we utilize $x_{i+1} - x_i = a$, a being the lattice constant (spacing between two consecutive lattice sites). Hence we derive the energy spectrum in terms of the wave-number as:

$$E(k) = t_R e^{ika} + t_L e^{-ika} = (t_R + t_L)\cos(ka) + i(t_L - t_R)\sin(ka), \qquad k = \frac{2\pi i}{L} \quad (i = 0, \ldots, L-1)$$

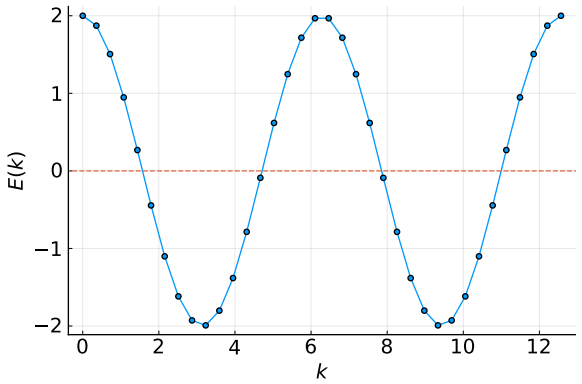

FIG. 2: Energy varying with k for the Hermitian Hatano-Nelson Model. The parameters taken are $a = 1, t = 1$

Note that, if $t_L = t_R = t$, then $E(k) = 2t\cos(ka) \in \mathbb{R}$ and the model becomes Hermitian, with real eigenvalues. However, if $t_L \neq t_R$, we will have a finite value for the imaginary part of the energy too.

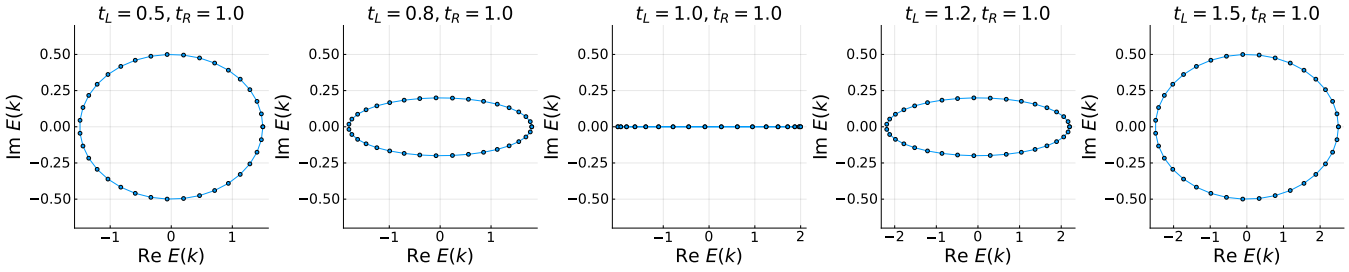

FIG. 3: For $t_L \neq t_R$, the imaginary and the real part as a function of k defines an ellipse and winds around the origin.

To this extent, we can define the spectral winding number for the system:

$$\omega = \frac{1}{2\pi i} \int_{-\pi}^{\pi} \mathrm{d}k \partial_k \ln E(k) = \begin{cases} +1, & |t_L| > |t_R| \\ -1, & |t_L| < |t_R| \end{cases}$$

From Figure. I, we cannot observe the orientation of the winding, however, the transition between the two windings is clear, since at $t_L = t_R$, the ellipses collapse and we have a flat line (since $\mathrm{Im}\, E(k) = 0$) In the equivalent

matrix representation under the periodic boundary and open chain case, we have the following:

$$[\hat{H}_{\text{HN}}]_{OBC} = \begin{pmatrix} 0 & t_L & 0 & 0 & \cdots \\ t_R & 0 & t_L & 0 & \cdots \\ 0 & t_R & 0 & t_L & \cdots \\ 0 & 0 & t_R & 0 & \cdots \\ \vdots & \vdots & \vdots & \vdots & \ddots \end{pmatrix} \qquad [\hat{H}_{\text{HN}}]_{PBC} = \begin{pmatrix} 0 & t_L & 0 & 0 & \cdots & t_R \\ t_R & 0 & t_L & 0 & \cdots & 0 \\ 0 & t_R & 0 & t_L & \cdots & 0 \\ 0 & 0 & t_R & 0 & \cdots & 0 \\ \vdots & \vdots & \vdots & \vdots & \ddots & \\ t_L & 0 & 0 & 0 & & \end{pmatrix}$$

Using exact diagonalisation, we can hence find the energy eigenvalues of the Hatano-Nelson Hamiltonian. Under open boundary condition, all the eigenstates of the Hatano-Nelson Model are exponentially localized on the boundary. The direction of localisation depends on the hopping term, that is, the states are localized on the left if $t_L > t_R$ and otherwise,on the right. This phenomenon is termed *non-Hermitian skin effect*.

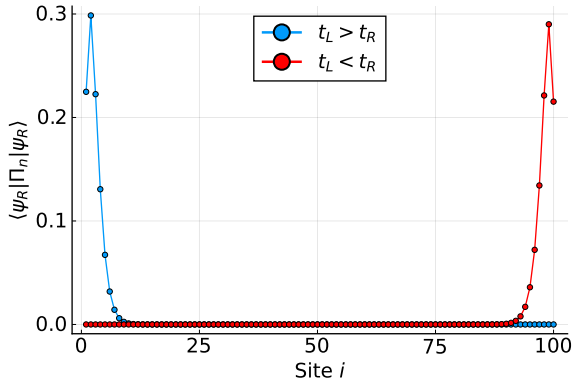

FIG. 4: Figure showing the localisation of states along the boundary. Parameters taken, for blue plot $t_L = 1.5, t_R = 0.5$ and for red plot $t_L = 0.5, t_R = 1.5$, $N = 100$.

For a non-Hermitian system, since $H^\dagger \neq H$, it is not guaranted that a state $|\psi\rangle$ satisfying $H|\psi\rangle = E|\psi_R\rangle$ will also satisfy the conjugate equation. Thus, we define two vectors for the Hamiltonian:

$$\begin{aligned} \text{Right Eigenvector:} \qquad & H|\psi_R\rangle = E|\psi_R\rangle \\ \text{Left Eigenvector:} \qquad & \langle\psi_L|H = E\langle\psi_L| \end{aligned}$$

Studying the left and right eigenvectors separately, we can observe the skin-effect. We also define the *biorthogonal localization* by:

$$C = \langle\psi_L|\Pi_n|\psi_R\rangle, \qquad \text{where } \Pi_n = c_n^\dagger|0\rangle\langle 0|c_n \text{ is the projector onto site } n$$

If the right eigenstate is localized to the right, the left eigenstate is localized to the left and hence the biorthogonal localisation nullifies this localisation, giving a 'bulk-state' picture in the biorthogonal formalism.

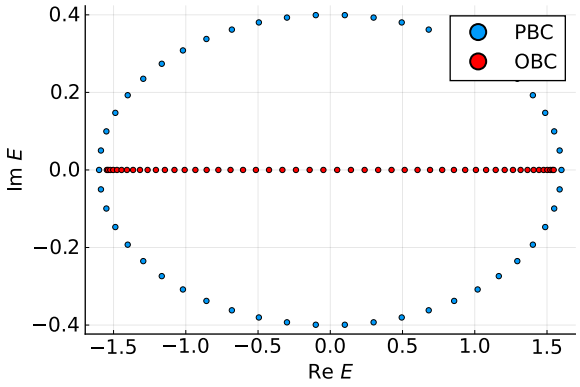

FIG. 5: Re E vs. ImE plot for both OBC and PBC case with parameters $N = 50, t_L = 0.6, t_R = 1.0$. We can see that while the PBC eigenvalues trace an ellipse, the OBC eigenvalues are purely real.

II. SSH MODEL

Let us start with the simplest topological model Hamiltonian known as the Su-Schrieffer-Heeger (SSH) model which has been used to describe polyacetylene or bi-partite/dimerized (Peierls) lattice [?] . The Hamiltonian reads

$$\begin{aligned}\hat{H}_{\text{SSH}} &= \sum_{I=1}^{L}[t + (-1)^I\delta]c_I^\dagger c_{I+1} \\ &= \sum_{i=0}^{L-1}(t+\delta)c_{A\,i}^\dagger c_{B\,i} + \sum_i (t-\delta)c_{A\,i+1}^\dagger c_{B\,i} + \text{h.c.} \\ &\equiv \sum_i [t_+ c_{A\,i}^\dagger c_{B\,i} + t_- c_{A\,i+1}^\dagger c_{B\,i} + \text{h.c.}]\,. \end{aligned} \tag{1}$$

Here the lattice consists of two different sublattice sites A and B inside each primitive cell as they associate with two different hopping amplitudes, namely $t_- = t - \delta$ (representing longer single bond having lesser kinetic energy or hopping for $\delta > 0$) and $t_+ = t + \delta$ (representing shorter double bond having higher kinetic energy or hopping for $\delta > 0$). t_+ and t_- are dubbed *intracell* and *intercell* hopping respectively.
Now the Hamiltonian can be written in the matrix form $\hat{H} = \mathbf{\Psi}^\dagger \mathbf{H} \mathbf{\Psi}$ with the basis (or spinor) $\mathbf{\Psi}^\dagger = [c_{A\,1}^\dagger c_{B\,1}^\dagger c_{A\,2}^\dagger \cdots]$. Then the Hamiltonian matrix becomes

$$\mathbf{H} = \begin{bmatrix} 0 & t_+ & 0 & \cdots & 0 \\ t_+^* & 0 & t_- & \cdots & 0 \\ \vdots & \vdots & \vdots & \vdots & 0 \\ 0 & 0 & 0 & t_{L-1}^* & 0 \end{bmatrix} \tag{2}$$

where the $(L-1)$-th hopping amplitude t_{L-1} is either t_+ or t_- depending on the value of L (even or odd).
Note that the above matrix represents the open boundary condition (OBC) where there exists no left-side hopping from cell 1 (considering cell 2 is on the right of cell 1) and no right-side hopping from cell L. However, if the periodic boundary condition (PBC) is applied, i.e. left-side hopping from cell 1 is the last cell L and right-side hopping from cell L finds the cell 1 back, then the Hamiltonian becomes

$$\mathbf{H} = \begin{bmatrix} 0 & t_+ & 0 & \cdots & t_L^* \\ t_+^* & 0 & t_- & \cdots & 0 \\ \vdots & \vdots & \vdots & \vdots & 0 \\ t_L & 0 & 0 & t_{L-1} & 0 \end{bmatrix} \tag{3}$$

To see a demonstration, take a simple example of a 4-site (2-cell) lattice (two A-sites + two B-sites) with OBC:

$$\mathbf{H}_{4\times4} = \begin{bmatrix} 0 & t_+ & 0 & 0 \\ t_+^* & 0 & t_- & 0 \\ 0 & t_-^* & 0 & t_+ \\ 0 & 0 & t_+^* & 0 \end{bmatrix} \tag{4}$$

Then

$$\begin{aligned} \hat{H}_{4\times4} &= \Psi^\dagger \mathbf{H}_{4\times4} \Psi \\ &= \begin{bmatrix} c_{A1}^\dagger & c_{B1}^\dagger & c_{A2}^\dagger & c_{B2}^\dagger \end{bmatrix} \begin{bmatrix} 0 & t_+ & 0 & 0 \\ t_+^* & 0 & t_- & 0 \\ 0 & t_-^* & 0 & t_+ \\ 0 & 0 & t_+^* & 0 \end{bmatrix} \begin{bmatrix} c_{A1} \\ c_{B1} \\ c_{A2} \\ c_{B2} \end{bmatrix} \\ &= \begin{bmatrix} c_{A1}^\dagger & c_{B1}^\dagger & c_{A2}^\dagger & c_{B2}^\dagger \end{bmatrix} \begin{bmatrix} t_+ c_{B1} \\ t_+^* c_{A1} + t_- c_{A2} \\ t_-^* c_{B1} + t_+ c_{B2} \\ t_+^* c_{A2} \end{bmatrix} \\ &= t_+ c_{A1}^\dagger c_{B1} + t_+^* c_{B1}^\dagger c_{A1} + t_- c_{B1}^\dagger c_{A2} \\ &\quad + t_-^* c_{A2}^\dagger c_{B1} + t_+ c_{A2}^\dagger c_{B2} + t_+^* c_{B2}^\dagger c_{A2} \,. \end{aligned} \tag{5}$$

III. RECIPROCAL SPACE REPRESENTATION

Now we want to write the Hamiltonian in the reciprocal (k) space. Again we can define the Fourier component of an annihilation operator:

$$c_{\alpha k} \equiv \frac{1}{\sqrt{L}} \sum_{i=1}^{L} e^{-ik.x_i} c_{\alpha i}; \quad \alpha = A, B \,. \tag{1}$$

[Note: We have total $2L$ lattice sites consisting of L number of A and B sublattices.]
Considering lattice coordinate at site i to be x_i with lattice spacing a (i.e., nearest neighbor site's position $x_{i+1} = x_i + a$), we can rewrite the Hamiltonian in Eq. (1):

$$\begin{aligned} \hat{H} &= \sum_i \sum_{kk'} \Big[\Big\{ t_+ c_{Ak}^\dagger c_{Bk} e^{ikx_i} e^{-ik'x_i} + \text{h.c.} \Big\} \\ &\quad + \Big\{ t_- c_{Ak}^\dagger c_{Bk} e^{ik(x_i+a)} e^{-ik'x_i} + \text{h.c.} \Big\} \Big] \\ &= \sum_{kk'} \Big[\Big\{ t_+ c_{Ak}^\dagger c_{Bk} \delta_{kk'} + \text{h.c.} \Big\} \\ &\quad + \Big\{ t_- c_{Ak}^\dagger c_{Bk} \delta_{kk'} e^{-ik'x_i} + \text{h.c.} \Big\} \Big] \\ &\qquad\qquad [\text{use } \textstyle\sum_i e^{i(k-k')x_i} = \delta_{kk'}] \\ &= \sum_k [\{ t_+ c_{Ak}^\dagger c_{Bk} + t_+^* c_{Bk}^\dagger c_{Ak} \} \\ &\quad + \{ t_- c_{Ak}^\dagger c_{Bk} e^{-ika} + t_-^* c_{Bk}^\dagger c_{Ak} e^{ika} \}] \\ &\equiv \sum_k H_k \,. \end{aligned} \tag{2}$$

Thus we get the momentum (k) dependent Hamiltonian (for simplicity, we consider the hopping parameters to be real, i.e. $t_+^* = t_+$, $t_-^* = t_-$)

$$H_k = t_+ (c_{Ak}^\dagger c_{Bk} + c_{Bk}^\dagger c_{Ak}) + t_- (c_{Ak}^\dagger c_{Bk} e^{-ika} + c_{Bk}^\dagger c_{Ak} e^{ika}) \tag{3}$$

$$= (t_+ + t_- e^{-ika}) c_{Ak}^\dagger c_{Bk} + (t_+ + t_- e^{ika}) c_{Bk}^\dagger c_{Ak} \,. \tag{4}$$

Like what we did in the direct lattice representation case, we choose a 2-dimensional spinor $\mathbf{\Psi}_k^\dagger \equiv [c_{Ak}^\dagger\, c_{Bk}]$ and write H_k in a 2×2 matrix form: $H_k = \mathbf{\Psi}_k^\dagger \mathbf{H}_k \mathbf{\Psi}_k$ where

$$\mathbf{H}_k \equiv \begin{bmatrix} 0 & t_+ + t_- e^{-ika} \\ t_+ + t_- e^{ika} & 0 \end{bmatrix}. \tag{5}$$

Then Eq. (4) can be written in the following form:

$$\mathbf{H}_k = d_x \boldsymbol{\sigma}_x + d_y \boldsymbol{\sigma}_y = \vec{d}(k).\vec{\sigma} \tag{6}$$

where $d_x(k) \equiv t_+ + t_- \cos ka$, $d_y(k) \equiv t_- \sin ka$; $\boldsymbol{\sigma}_x = \begin{bmatrix} 0 & 1 \\ 1 & 0 \end{bmatrix}$ and $\boldsymbol{\sigma}_y = \begin{bmatrix} 0 & -i \\ i & 0 \end{bmatrix}$.

IV. DIGRESSION: BERRY PHASE

The Bloch wave function is not unique: $|u_\mathbf{k}\rangle \to e^{i\phi(\mathbf{k})}|u_n, \mathbf{k}\rangle$ is invariant under the gauge transformation $\mathbf{A} \to \mathbf{A} + \boldsymbol{\nabla}_\mathbf{k}\phi(\mathbf{k})$ where

$$\mathbf{A} = i\langle u_\mathbf{k}|\boldsymbol{\nabla}_\mathbf{k} u_\mathbf{k}\rangle \tag{1}$$

is known as the *Berry connection* (analogous to the magnetic vector potential). For any close loop C in the $\mathbf{k}$-space, the Berry phase can be defined as

$$\gamma_C = \oint_C \mathbf{A}.d\mathbf{k} = \int_S \mathcal{F} d^2\mathbf{k} \tag{2}$$

where $\mathcal{F} \equiv \boldsymbol{\nabla} \times A$ is known as the *Berry curvature*.
For a TLS Hamiltonian $H(\mathbf{k}) = \vec{d}(\mathbf{k}).\vec{\sigma}$, Berry showed[?] [*to be shown]

$$\gamma_C = \Omega/2 \tag{3}$$

where Ω is the solid angle swept out by $\hat{d}(\mathbf{k})$.

V. DIGRESSION: TWO LEVEL SYSTEM

In general a two-level Hamiltonian can be written as

$$\hat{H}_0 = E_1|1\rangle\langle 1| + E_2|2\rangle\langle 2| \tag{1}$$

The Hamiltonian in the matrix form becomes

$$H_0 = \begin{bmatrix} E_1 & 0 \\ 0 & E_2 \end{bmatrix} \tag{2}$$

Now if we turn on an interaction V between state $|1\rangle$ and $|2\rangle$, we get an interacting Hamiltonian

$$\hat{H} = E_1|1\rangle\langle 1| + E_2|2\rangle\langle 2| + V|1\rangle\langle 2| + V^*|2\rangle\langle 1| \tag{3}$$

which gets the matrix form

$$\mathbf{H} = \begin{bmatrix} E_1 & V \\ V^* & E_2 \end{bmatrix} \tag{4}$$

The eigenvalue equation becomes

$$(E_1 - E)(E_2 - E) - |V|^2 = 0 \tag{5}$$

which yields two eigenvalues E_+ and E_- given by

$$E_\pm = (E_1 + E_2) \pm \sqrt{(E_1 - E_2)^2 + 4|V|^2}\,. \tag{6}$$

Suppose we have the following Hamiltonian

$$\mathbf{H}(k) = \begin{bmatrix} h_0 + h_z & h_x - ih_y \\ h_x + ih_y & h_0 - h_z \end{bmatrix} \tag{7}$$

Then the Hamiltonian can be written as

$$H(k) = h^\mu(k)\sigma_\mu = h_0(k)\mathbb{1} + \vec{h}(k).\vec{\sigma} \tag{8}$$

where $\mathbb{1}$ is the 2×2 unity matrix.
With $\mathrm{Tr}(H) = 2h_0$ and $\det(H) = h_0^2 - h^2$, one finds the eigenvalues

$$E_\pm = h_0 \pm h(k) \tag{9}$$

where

$$h(k) = ||\vec{h}(k)|| = \sqrt{h_x^2 + h_y^2 + h_z^2}\,. \tag{10}$$

The corresponding normalized eigenvectors are (up to a phase factor)

$$u_\pm(k) = \frac{1}{\sqrt{1 + (h_z + E_\pm^2)/(h_x^2 + h_y^2)}} \begin{bmatrix} E_\pm/(h_x + ih_y) \\ 1 \end{bmatrix}. \tag{11}$$

VI. BACK TO THE SSH MODEL

Dispersion:

Now if we compare our k-space SSH Hamiltonian in Eq. (6), we notice h_0 and $\vec{h}(k) = \vec{d}(k)$. Therefore from Eq. (9)

$$\begin{aligned} E_k &= \pm|\mathbf{d}(k)| = \pm\sqrt{(t_+ + t_- \cos ka)^2 + t_-^2 \sin^2 ka} && (1) \\ &= \pm\sqrt{(t_+ - t_-)^2 + 4t_+t_- \cos^2(ka/2)} \\ &= \pm\sqrt{(4\delta^2 + 4t_+t_- \cos^2(ka/2)}\,. && (2) \end{aligned}$$

with $d_x(k) \equiv t_+ + t_- \cos ka$, $d_y(k) \equiv t_- \sin ka$.

Other Nomenclatures:

In many literatures, the intracell hopping $t_+ = t + \delta$ is denoted by v and intercell hopping $t_- = t - \delta$ is denoted by w. Now onward, we shall follow this notation and according to it,

$$d_x(k) \equiv v + w \cos ka; \quad d_y(k) \equiv w \sin ka \tag{3}$$

and

$$E(k) = \pm\sqrt{v^2 + w^2 + 2vw \cos ka}\,.$$

From Eq. (3), we get

$$(d_x - v)^2 + d_y^2 = w^2 \tag{4}$$

which describes a circle of radius w, centered at $(v, 0)$.
?

VII. WINDING NUMBER (ν): THE RUBBER BAND ANALOGY

Winding number is a many times a curve winds around a specific point z_0.
Our case: $z_0 = (d_x = 0, d_y = 0)$ $\nu = 1$ is topologically non-trivial!
The winding number can be mathematically formualated as [Check derivation!]:

$$\nu = \frac{1}{2\pi}\int_{-\pi}^{\pi} dk \left(\hat{\mathbf{d}}(k) \times \frac{d}{dk}\hat{\mathbf{d}}(k)\right)_z . \tag{1}$$

When the intracell hopping dominates over the intercell hopping (i.e. $v > w$), the winding number $\nu = 0$. On the other hand, when $v < w$, $\nu = 1$. to change ν, we need to change the path of $\mathbf{d}(k)$

Formula 4

Since $E(k) = \pm|\mathbf{d}(k)|$, we have

$$\begin{aligned} \ln E(k) &= \ln|\mathbf{d}(k)| + i\arg(\mathbf{d}(k)) . \\ \Rightarrow \partial_k \ln E(k) &= \partial_k \ln|\mathbf{d}(k)| + i\partial_k \arg(\mathbf{d}(k)) . \end{aligned} \tag{2}$$

Now we know

$$\nu = \frac{1}{2\pi}\oint_C \partial_k \arg(\mathbf{d}(k)) \quad [\text{see above}] . \tag{3}$$

Also,

$$\nu = \frac{1}{2\pi i}\oint_C dk\, \partial_k \ln E_k . \tag{4}$$

Also,

$$\nu = \frac{i}{2\pi}\int_{C_\beta} dq\, q^{-1}. \tag{5}$$

VIII. EDGE STATES

2 degenerate $E = 0$ bands

- Edge states function as connectors/interfaces between 2 toplogical distinct phases [trivial ($\nu = 0$) and non-trivial ($\nu = 1$)] $\Rightarrow$ Bulk-boundary correspondence (BBC).

1. Shen: Topolgical Insulator and Dirac Equation in Condensed Matter
2. http://optics.szfki.kfki.hu/~asboth/topins_course/2015-09-24-ELTE-Topins.pdf
3.

IX. NON-HERMITIAN TOPOLOGICAL INSULATORS

Hamiltonian in direct space

$$\begin{aligned} \hat{H} = B\sum_i (t_1 - \gamma/2)\, c^\dagger_{A\,i} c_{B\,i} + \sum_i (t_1 + \gamma/2)\, c^\dagger_{B\,i} c_{A\,i} \\ + \sum_i t_2[c^\dagger_{A\,i+1} c_{B\,i} + c^\dagger_{B\,i} c_{A\,i+1}] + \sum_i t_3[c^\dagger_{A\,i} c_{B\,i+1} + c^\dagger_{B\,i+1} c_{A\,i}] . \end{aligned} \tag{1}$$

?

REFERENCES